JOURNAL OF SOLID STATE CHEMISTRY **131,** 189–197 (1997)
ARTICLE NO. SC977269

Structural and Spectroscopic Evidence for Hydrogen Bonding Induced NH_4^+ Cation Ordering in β-$(NH_4)_2FeF_5$ at Low Temperature

L. Croguennec,* P. Deniard,* R. Brec,* M. Couzi,† C. Sourisseau,† J. L. Fourquet,‡ and Y. Calage‡

** Laboratoire de Chime des Solides, Institut des Matériaux de Nantes, B. P. 3229, 44322 UM 110 CNRS, 2 rue de la Houssinière, Nantes Cedex 03, France;*
† Laboratoire de Spectroscopie Moléculaire et Cristalline, URA 124 CNRS, Université de Bordeaux I, 351 cours de la Libération,
33405 Talence Cedex, France; and ‡ Laboratoire des Fluorures, URA 449 CNRS, Faculté des Sciences, Université du Maine,
72017 Le Mans Cedex, France

Received April 17, 1996; in revised form December 24, 1996; accepted January 7, 1997

An X-ray Rietveld structure determination of β-$(NH_4)_2FeF_5$ at 133 K showed that the transition, observed at 133 K on the parameter versus temperature curve, corresponds to the ordering of one of the two NH_4^+ cations of the compound. The structure calculations could be carried out successfully thanks to the use of the rigid body approach, which considers collectively the four hydrogen atoms of the NH_4^+ group, assumed to retain a tetrahedral symmetry. Very short H ··· F distances of 1.88 Å are observed that correspond to strong hydrogen bonding between the NH_4^+ groups and the $[FeF_5]^-$ chain. This results in the straightening of the corrugated fluoride chain. A Raman spectroscopic study confirmed the occurrence of the transition through high and low frequency spectrum recording. At low temperature, the Raman bands become narrower and/or split into several components. In the high frequency domain, an increase of a new component at about 3082 cm^{-1} proves clearly the setting up of stronger hydrogen bonding around 133 K. The peaks at higher frequencies (3280, 3197, and 3119 cm^{-1}) present a weak intensity, in agreement with the presence of the disordered NH_4^+ cation, as found by the structure determination.

I. INTRODUCTION

In many compounds containing molecules of NH_3, H_2O, or hydrocarbon groups such as $-CH_3$ or $-C_2H_5$, one finds either static or dynamic disorder of these molecules at high temperature. This is also often the case for hydrogen-containing cations such as NH_4^+ and Et_4N^+. In the case of dynamic disorder, lowering the temperature is expected to result in freezing out of the molecules in energetically favorable orientations. It is then possible to refine the hydrogen positions when the structure determination is carried out from a single crystal, even if the atomic displacement parameters (ADP) have to be arbitrarily fixed. It is much more difficult to perform the same work when only polycrystalline material is available. This is the actual situation for the β-$(NH_4)_2FeF_5$ phase, which is obtained as a powder by dehydration of $(NH_4)_2FeF_5 \cdot H_2O$ above 371 K (1, 2). Up to now, only the room temperature Rietveld refinement of this phase has been performed (2), without the hydrogen positions of the NH_4^+ cations being taken into account, these groups being considered as disordered. Following a DSC observation that a transition was taking place around 187.1 K, a spectroscopic low temperature study of β-$(NH_4)_2FeF_5$ was undertaken on polycrystalline samples of the compound. Also, because the transition was assumed to be related to NH_4^+ cation ordering, a full refinement of the structure including hydrogen positions was attempted with the help of the rigid body technique, leading to meaningful results. The ordering of only one of the two ammonium groups of β-$(NH_4)_2FeF_5$ could be thus confirmed by two independent experimental techniques: X-ray diffraction Rietveld refinement and Raman spectroscopy.

II. EXPERIMENTAL

II.1. Diffraction

β-$(NH_4)_2FeF_5$ was prepared by dehydration of β-$(NH_4)_2FeF_5,H_2O$ according to the procedure described in (2). The phase was pure and found to correspond well to the previously published room temperature structural data ($a = 6.3385(3)$ Å, $b = 7.6191(2)$ Å, $c = 11.0298(4)$ Å in the present study versus $a = 6.3379(6)$ Å, $b = 7.6165(5)$ Å, $c = 11.0305(9)$ Å in the previous one) with parameters overlapping within three times the estimated standard deviations.

Powder diffraction diagrams were recorded on a Siemens 5000 diffractometer (filtered Cu$K\alpha$ radiation) in a Bragg–Brentano geometry. Powder of grain size 20 μm was deposited in a cavity at the surface of a flat plate and gently leveled using a frosted glass plate to minimize preferred orientation. The data were collected in steps of 0.03° (2Θ) with 190-sec counting periods over a 10°–120° range (2Θ). The powder patterns were processed with the Prolix program (3)

0022-4596/97 $25.00

including several options such as background stripping, peak search, and profile fitting. The Rietveld calculations were carried out using the program Fullprof (4) in a first step and then the rigid body calculation approach from the GSAS package (5) was taken, using the Thompson–Cox–Hastings function for profiles and a cosine Fourier series for background. The low temperature diagrams were recorded in the 300 K–130 K temperature range with the low temperature attachment provided by Siemens.

II.2. Raman Spectroscopy

The samples were introduced, in an argon dry box, into small thin-walled glass capillaries that were subsequently sealed. The spectra were recorded with a triple monochromator (Dilor Z24 model) with the 5145 Å wavelength of an ionized argon laser used at low power ($I_0 < 30$ mW). A liquid nitrogen cryostat was used to explore temperatures from 300 K to 100 K. The two characteristic 30–700 cm^{-1} and 2400–3400 cm^{-1} wavenumber domains were probed.

III. RESULTS AND DISCUSSION

III.1. X-Ray Diffraction Study

The X-ray study involved recording the powder diagrams of β-$(NH_4)_2FeF_5$ to observe the orthorhombic cell parameter changes with temperature and to confirm the structural transition. The structure was then refined to determine the crystallographic nature of this transformation. The peak indexing and the refinement of the cell parameters were performed in the *Pnma* ($Z = 4$) space group without any particular problem. No peaks remained unaccounted for. This means that no symmetry change (space group modification and/or occurrence of superstructure) could be detected at the X-ray powder diffraction level.

Figure 1 shows the *a*, *b* and *c* parameter evolution versus *T*. On the three curves a transition is detected through break recorded at about 193 K, a value close to that determined from a DSC study (187 K) (7).

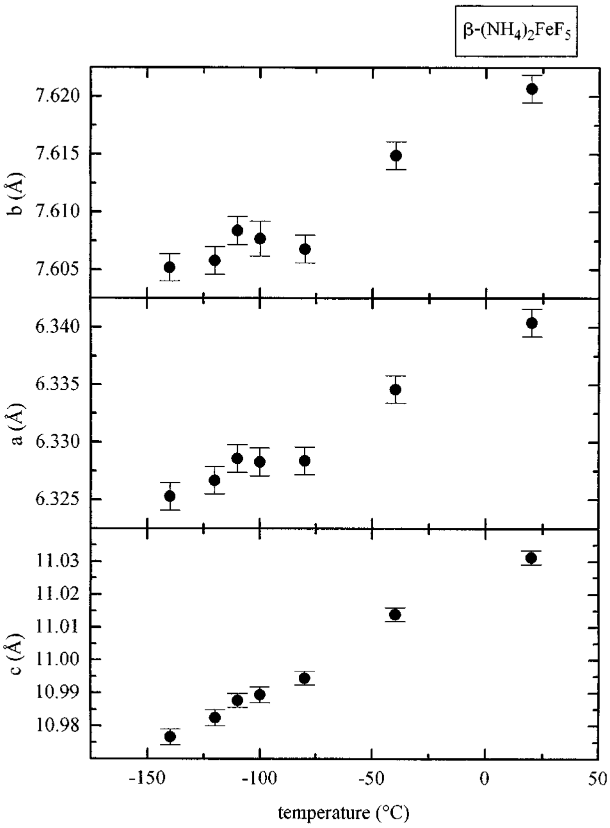

FIG. 1. Changes of the cell parameters of β-$(NH_4)_2FeF_5$ versus temperature in the 298–133 K range. A break in the curves is recorded at about 193 K, indicating a phase transition, in agreement with a previous DSC study.

Rietveld refinements of the atomic structure (all atoms with isotropic ADPs) were then performed on the different temperature data using the *Pnma* space group and the atomic position determined earlier. Again, the results were consistent with the previous study, without important or obvious changes. To take into account the four hydrogens around nitrogen and as found before (2), the first calculations refined the occupancy ratio τ of the nitrogen positions: τ increased from 1 to 1.32, and the refinement converged with a meaningful lowering of the goodness of fit as compared to the refinement when τ was equal to one, indicating that the powder diagram quality was good enough to be sensitive to the four hydrogen electron contribution. From this step, it was decided to use the rigid body approach (5), the NH_4^+ groups being considered as perfect tetrahedral units with ideal H–N–H angles of 109.47° and N–H distances of 1 Å. The two NH_4^+ tetrahedral groups of β-$(NH_4)_2FeF_5$ were only allowed to rotate around nitrogen as their centers. A first calculation made on the room temperature diagram did not find any ordering of NH_4^+, the H atomic displacement parameter remaining very high (50 $Å^2$). By contrast, the low temperature diagram refinement showed an ordering of one of the NH_4^+ group (N2 site). It appeared that the hydrogen positions of the N2 site refined staisfactorily, whereas very high ADPs were obtained for the hydrogen positions for the N1 site ($B_{iso} =$ 40 $Å^2$), suggesting that this group remained disordered. Calculations were then resumed by refining the τ occupation ratio as done before for the room temperature structure. Also, since the B_{iso} values of the N2 hydrogen atoms were slightly negative (-0.2 $Å^2$), a more realistic value of 2.5 $Å^2$ was chosen and fixed for these atoms. From now on, the results reported are going to be those of the lowest temperature study, i.e., 133 K. The final atomic positional parameters and data of the refinement are given in Table 1 with, for the sake of comparison, room temperature data obtained from

TABLE 1
Atomic Positional Parameters of β-$(NH_4)_2FeF_5$ as Calculated from a Rietveld Refinement at 133 K

		x	y	z	B_{iso}
N1	4c	0.442(4) [0.428(1)]	1/4	0.198(3) [0.1958(9)]	2.3(1) [5.4(3)]
N2	4c	0.512(4) [0.510(1)]	1/4	0.854(3) [0.8584(9)]	3.6(1) [4.9(2)]
Fe	4c	0	0	0	1.6(1) [0.74(2)]
F1	4c	0.081(1) [0.0880(6)]	1/4	– 0.002(2) 0.0082(6)	0.6(3) [1.6(1)]
F2	8d	0.225(2) [0.2271(7)]	0.045(1) [0.0521(5)]	0.442(1) [0.4367(5)]	2.1(4) [2.7(1)]
F3	8d	0.102(2) [0.1051(8)]	0.546(2) [0.5265(7)]	0.163(1) [0.1595(4)]	4.1(5) [2.9(1)]
H1	8d	0.426(7)	0.3573	0.872(8)	2.5
H2	4c	0.64(1)	1/4	0.90(1)	2.5
H3	4c	0.55(2)	1/4	0.766(5)	2.5

Note. B_{iso} for H atoms are fixed at a reasonable value based on the atomic mass of hydrogen. As H2 and H3 atoms are constrained to be on the same mirror and belong to the same rigid body as H1, the y coordinate for the latter is also constrained in the y direction (this explains why the H1 ESD is not reported). The same values for the room temperature study are found between brackets.

(2). In Table 2 can be found the main interatomic distances. Figure 2 gives the Rietveld profiles obtained at the end of the refinement procedure with and without the rigid body model ($R_{wp} = 0.013$, $R_B = 0.048$, and $\chi^2 = 0.16$). Figure 3 features the overall location of the ordered and disordered ammonium cations.

III.2. Structure Discussion

First of all, it is to be pointed out that all the atoms see their B_{iso} values decrease with temperature, except Fe and F3 (Table 1). However, the difference is meaningless for F3 since for this atom the B_{iso} value has a rather large ESD. There is no obvious explanation for that of Fe, unless an undetected structural change has occurred, with a departure of iron from the special position. However, a Mössbauer study found two different sites at low temperature (see below), and the high ADP may account for two iron positions. F1, the bridging fluorine between two $[FeF_6]$ octahedra, keeps a low ADP (it was the lowest value among the room temperature fluorine atoms). Within error, the mean Fe–F distance remains identical to that of the room temperature one (Table 2).

TABLE 2
Main Atomic Distances in β-$(NH_4)_2FeF_5$ at 133 K

Fe	F3	F3	F2	F2	F1	F1
F3	**1.94(1)**	3.87(3)	2.67(1)	2.74(1)	2.62(2)	2.89(2)
F3	180.0	**1.94(1)**	2.74(1)	2.67(1)	2.89(2)	2.62(2)
F2	91.521	88.479	**1.89(1)**	3.77(2)	2.82(1)	2.63(1)
F2	88.479	91.521	180.0	**1.89(1)**	2.63(1)	2.82(1)
F1	95.587	84.413	84.413	86.072	**1.969(2)**	3.938(5)
F1	84.413	95.587	95.587	93.928	180.0	**1.969(2)**

$a = 6.3269(5)$, $b = 7.6076(2)$, $c = 10.9802(9)$, space group *Pnma*

N1 polyhedron		N2 polyhedron	
2 × F2	2.82(2)	2 × F3	2.70(3)
2 × F3	2.90(3)	2 × F2	2.86(2)
2 × F3	3.14(2)	2 × F3	2.90(2)
F1	3.17(4)	2 × F2	3.05(4)
		F1	3.16(3)
⟨N1–F⟩ = 2.985		⟨N2–F⟩ = 2.909	

H1		H2		H3	
F2	1.88(3)	F2	2.35(8) × 2	F3	2.16(9) × 2
F3	2.42(9)	F3	2.36(8) × 2	F3	2.79(9) × 2
F1	2.71(3)	F1	2.96(5)	F1	2.91(5)
F2	2.88(9)				

The ordering of the NH_4^+ group (Fig. 4) leads to two short H1–F2 distances of 1.88(3) Å, a length sufficiently small to give rise to rather strong hydrogen bonding. The other distances are much longer (H1–F3 = 2.42(9) Å, H1–F1 = 2.71(3) Å, and H1–F2 = 2.88 Å), giving substantially weaker $H \cdots F$ interactions (see below the spectroscopic study confirming these features).

The strong hydrogen bonding induces a flattening of the Fe–F1–Fe angle from 148° at ambient temperature (2) to 150° at 133 K. This agrees well with the occurrence of two successive $[FeF_6]$ titled octahedra bonded via H1 to two successive NH_4^+ groups (Fig. 4).

IV. RAMAN STUDY

IV.1. Selection Rules

Under the assumption of the *Pnma* (or D_{2h}^{16}) space group with a multiplicity of $Z = 4$, quite a large number of vibrational modes are expected:

With two independent NH_4^+ ammonium groups located on (4c) or ($\sigma(xz)$) sites, the correlation table between $T_d \leftrightarrow C_s \leftrightarrow D_{2h}$ groups shows that all the modes are infrared and Raman active, through intermolecular effects, with splittings into four components ($A_g + B_{2g} + B_{1u} + B_{3u}$) or

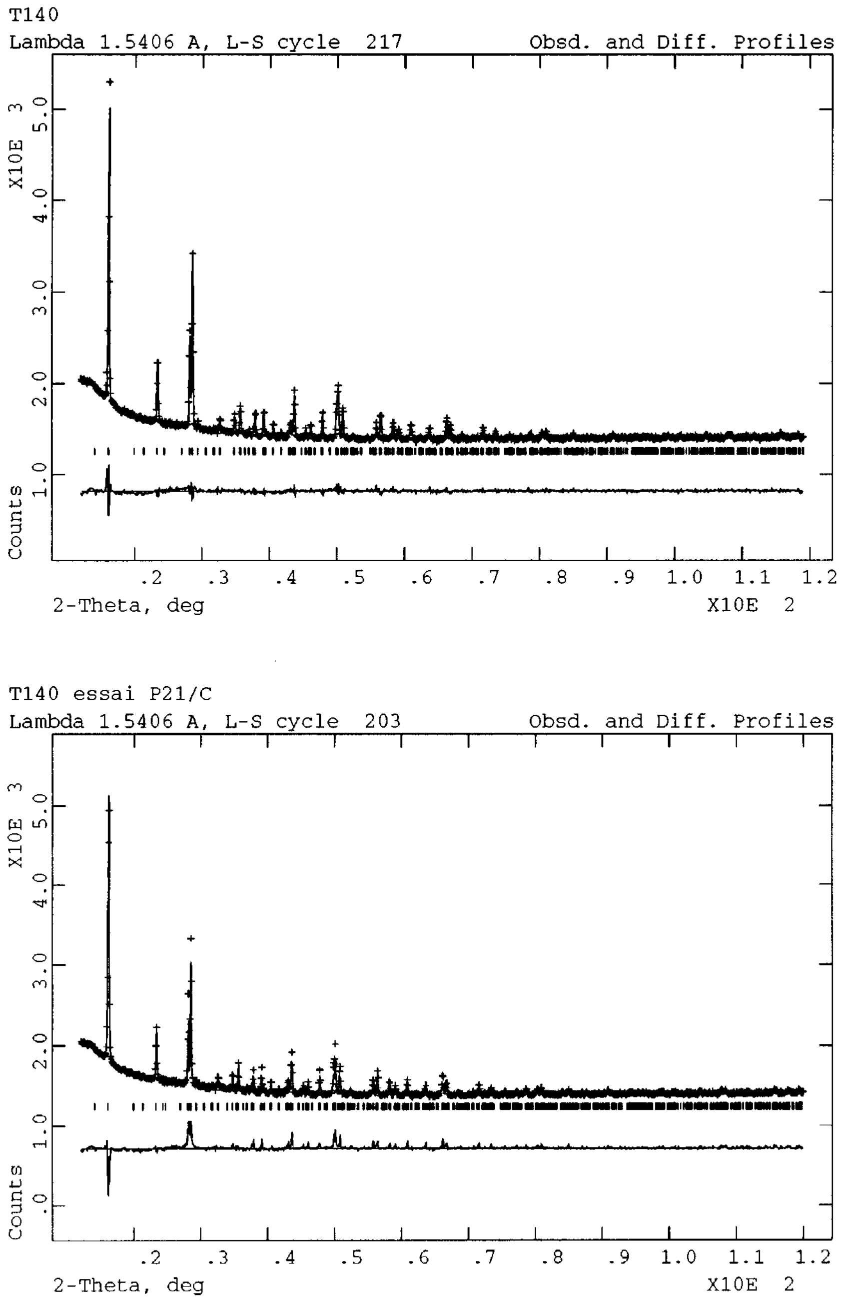

FIG. 2. Results of the 133 K X-ray diffraction Rietveld analysis of β-$(\mathrm{NH}_4)_2\mathrm{FeF}_5$. The first curve (top) represents the final result with the rigid body approach allowing for the refinement of an $[\mathrm{H}_4]$ tetrahedron around N2. The second curve (bottom) shows the same calculation without taking into account the order of $\mathrm{N2(H_4)}^+$. The fit difference demonstrates clearly the occurrence of the ordering and justifies the use of the technique.

$(B_{1g} + B_{3g} + (A_u) + B_{2u})$. This corresponds to

$$\Gamma\, 8\times(\mathrm{NH}_4^+) = \underbrace{18A_g + 12B_{1g} + 18B_{2g} + 12B_{3g}}_{\text{Raman}} + \underset{\text{in.}}{(12A_u)} + \underbrace{18B_{1u} + 12B_{2u} + 18B_{3u}}_{\text{IR}}. \qquad [1]$$

Fe^{3+} ions are on (4a) or C_i sites and give, via the $C_i \leftrightarrow D_{2h}$ correlation,

$$\Gamma\, 4\times(\mathrm{Fe}^{3+}) = (3A_u) + 3B_{1u} + 3B_{2u} + 3B_{3u}.$$

The fluorines of type F2 and F3 are in the (8d) or C_1 general position, hence,

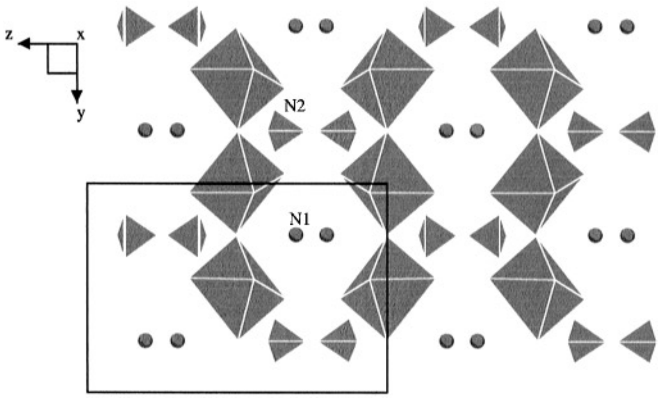

FIG. 3. Perspective view of the structure of low temperature β-$(NH_4)_2FeF_5$. The tetrahedra are the ordered $N2(H_4)^+$ groups whereas the small spheres represent the disordered $N1(H_4)^+$ ammonium cations.

$$\Gamma\, 4\times(\mathrm{F2, F3}) = 6A_g + 6B_{1g} + 6B_{2g} + 6B_{3g} + (6A_u) + 6B_{1u} + 6B_{2u} + 6B_{3u}.$$

Finally, the F1 fluorine atoms are in the (4*c*) or $\sigma(xz)$ sites with

$$\Gamma\, 4\times(\mathrm{F1}) = 2A_g + 1B_{1g} + 2B_{2g} + 1B_{3g} + (1A_u) + 2B_{1u} + 1B_{2u} + 2B_{3u}.$$

That is, in all,

$$\Gamma\, 4\times(\mathrm{FeF_5}) = 8A_g + 7B_{1g} + 8B_{2g} + 7B_{3g} + (10A_u) + 11B_{1u} + 10B_{2u} + 11B_{3u}. \qquad [2]$$

To obtain the number of expected spectroscopic peaks, one has to subtract the three acoustic modes from the relations [1] and [2]. Then

$$\Gamma(\mathrm{Total}) = \underbrace{26A_g + 19B_{1g} + 26B_{2g} + 18B_{3g}}_{90\ \mathrm{Raman}} + \underset{\mathrm{in.}}{(22A_u)} + \underbrace{28B_{1u} + 21B_{2u} + 28B_{3u}}_{77\ \mathrm{IR}}.$$

IV.2. Results and Discussion

The 30–700 cm^{-1} low frequency domain. In this region, 15 Raman active modes are expected from $[FeF_5]^{2-}$ anions (Eq. [2]), plus 12 Raman modes related to the *R*' librations $(1A_g + 2B_{1g} + 1B_{2g} + 3B_{3g})$ and to the T′ translations $(2A_g + 1B_{1g} + 2B_{2g} + 1B_{3g})$ of the NH_4^+ cations.

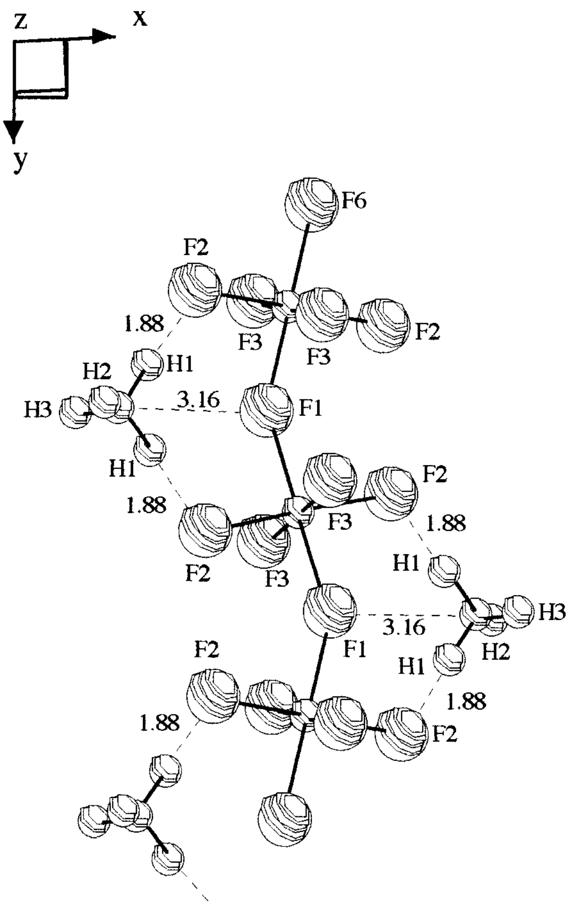

FIG. 4. Portion of the $[FeF_5]^{2-}$ chains in β-$(NH_4)_2FeF_5$ with the hydrogen-bonding $N2(H_4)^+$ groups showing the short H1 ··· F2 distances responsible of the bonds.

The experimental observations show clearly that we are far from that number since only 8 signals at ambient temperature and 13 signals at 100 K are observed (Fig. 5 and Table 3), this including very weak bands and shoulders. From a spectroscopic standpoint, one would expect actually a higher symmetry and/or a smaller cell. However, the sample under study proved a very poor scatterer (like most inorganic fluorides) and therefore we detect only the strongest bands due to the totally symmetrical modes (A_g). In addition, in partially disordered structures, the low frequency region reflects only a mean situation of the crystals.

Upon cooling, numerous Raman bands become narrower and/or split into several components, their wavenumber expectedly increasing by a few cm^{-1} (from 4 to 8 cm^{-1}). However, it is important to notice the abnormal behavior of the 172 cm^{-1} mode (at 300 K), which first splits into two bands at 166 and 190 cm^{-1} (at 150 K) and then leads to at least three components at 172, 192, and 205 cm^{-1} (at 100 K). For the two last, this represents important shifts indicative of strong constraints at low temperature, with distortions perpendicular to the b axis (in the ac plane)

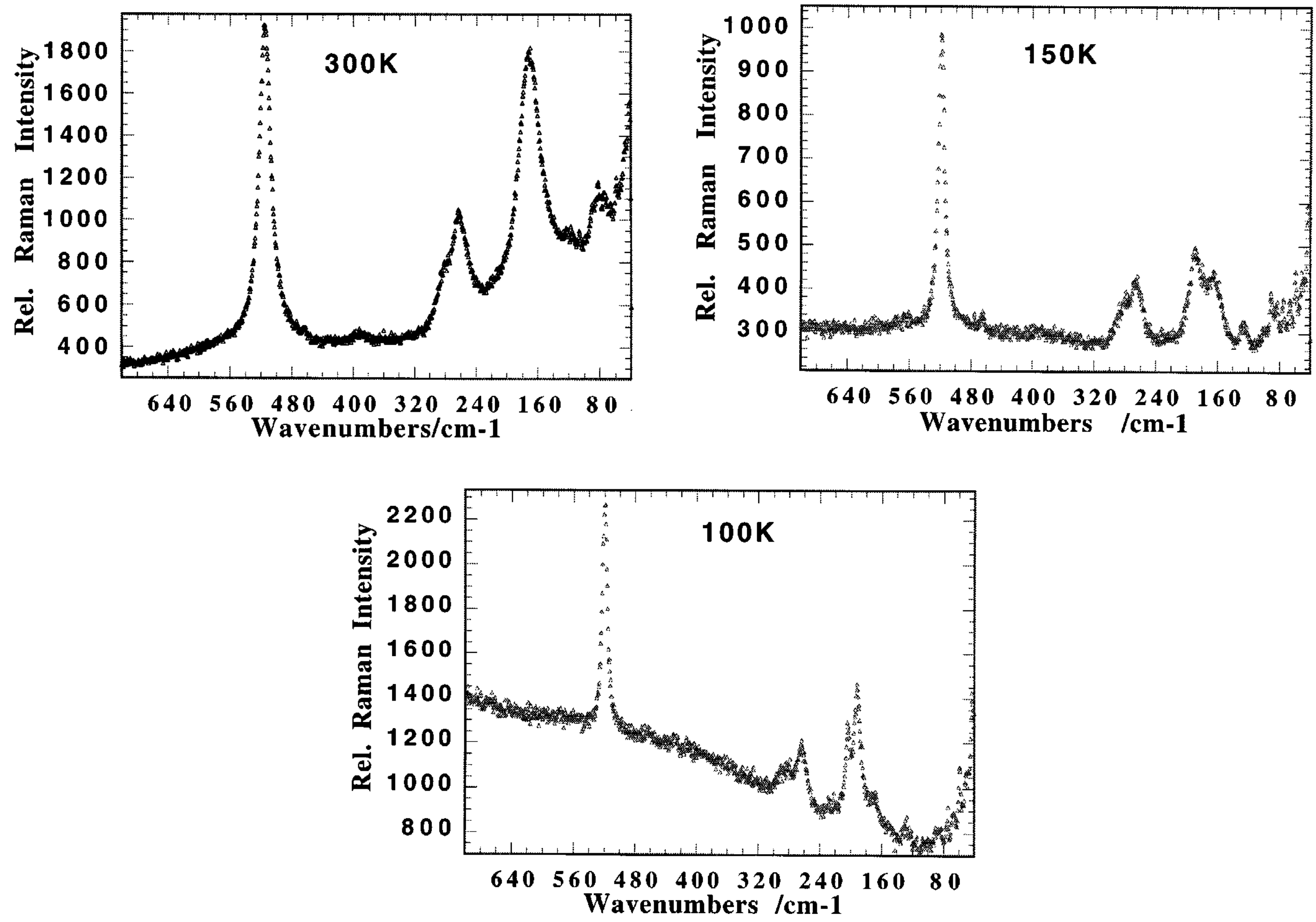

FIG. 5. Low frequency domains of the Raman spectra of β-$(NH_4)_2FeF_5$ recorded between 300 and 110 K.

i.e. perpendicular to the $[FeF_5]^{2-}$ chains. The mode at $172\,cm^{-1}$ has no equivalent in compounds containing isolated FeF_6 groups, whereas modes at 515 and $264\,cm^{-1}$ can be related respectively to the stretching and deformation vibrations of an XY_6 octahedron (ν_1, A_{1g} and ν_5, F_{2g}) (6). Clearly, this new band is to be related to the Fe–F2 and Fe–F3 bonds (Fig. 4) involved in a deformation with a strong component perpendicular to the $[FeF_5]^{2-}$ chains.

The 3000–3400 cm^{-1} high frequency domain. In this domain, ν N–H stretching vibrations are expected. They originate from the ν_1 (A_1 in T_d) and ν_3 modes (F_2 in T_d) of the NH_4^+ tetrahedra, that is, normally a total of 16 active modes in Raman ($6A_g + 2B_{1g} + 6B_{2g} + 3B_{3g}$).

The 300 K spectrum shows only a very wide band (Fig. 6 and Table 4), nonsymmetric and centered around $3133\,cm^{-1}$ with shoulders at higher frequencies at about 3208 and $3262\,cm^{-1}$. In agreement with the room temperature structure determination, this indicates the occurrence of a wide hydrogen bonding distribution (due to disordered NH_4^+ groups) from medium (2.88–2.90 Å) to weak (3.0–3.14 Å).

Upon temperature lowering (200 to 168 and to 150 K), the wide band becomes better defined, with a decrease of the intensities at high frequencies and an increase of a new component at lower frequency around $3082\,cm^{-1}$ (see Fig. 6 and Table 4). This clearly proves the setting up of stronger hydrogen bonds around 150 K.

Finally, the 110 K spectrum shows that the phenomenon recorded at 150 K is amplified, since the 3095, 3084, and $3066\,cm^{-1}$ components are very intense and notably narrow. This confirms a real reinforcement of the N–H$\cdots$F bonding. Also, and as reported earlier from DTA analyses, all these effects are reversible. We also note that the peaks located at higher frequencies, corresponding to weaker bonding (3280, 3197, and $3119\,cm^{-1}$ for the 110 K spectrum), present a weak intensity. All these observations are in agreement with the presence of an ordered and a disordered NH_4^+ cation, as found in the low temperature structure determination (see above).

TABLE 3
Low-Frequency Raman Data in β-$(NH_4)_2FeF_5$ at Various Temperatures

300 K (ν/cm^{-1})	150 K (ν/cm^{-1})	100 K (ν/cm^{-1})	$\Delta\nu$ (100 K 300 K)	Tentative assignments
~ 84 m bd	~ 88 mw	88 w	+ 4	Lattice modes (T' NH_4^+ ?)
120 m	128 mw	128 w	+ 8	
172 s	166 ms	173 m	+ 1	FeF_6^{3-} chain deformations in the (ac) plane
—	190 ms	192 ms	+ 20	
	—	205 ms	+ 33	
—	228 vw	228 vw		
264 s	266 ms	265 ms	+ 1	FeF_6^{3-} internal bending (ν_s)
	278 m	279 m	+ 8	
281 sh	288 sh	291 sh	+ 10	
394 wv bd	~ 395 vw bd	~ 394 vw bd	0	$R'NH_4^+$ or FeF_6^{3-} internal stretching (ν_2)
463 vw	465 vw	464 vw	+ 1	ν_{sym} F_1–Fe–F_1?
	506 sh	506 sh		FeF_6^{3-} sysm. stretching (ν_1)
516 vs	520 sh	520 vs	+ 4	

Note. m: medium; ms: medium sharp; mw: medium weak; bd: broad; s: sharp; vs: very sharp; sh: shoulder; w: weak; vw: very weak.

We cannot go further in the spectral analysis since we observe significant overlapping of all the ν_1 and ν_3 components of the NH_4^+ groups which correspond to at least three types of N–H bonds involved in different hydrogen bonding situations. Furthermore, the temperature dependence of the Raman spectra in this region looks like a continuous evolution of increased hydrogen bonding and ordering below the transition temperature.

V. CONCLUDING REMARKS

The structural and spectroscopic studies performed on β-$(NH_4)_2FeF_5$ at 133 K demonstrate clearly the ordering of one of the two NH_4^+ groups of the structure and the subsequent implementation of stronger H $\cdots$ F bonding. Owing to these stronger and well localized hydrogen bonds, a strain is observed on the chain octahedra, with a marked

TABLE 4
Raman Data in the ν–N–H Frequency Range for β-$(NH_4)_2FeF_5$ at Various Temperatures

300 K (ν/cm^{-1})	200 K (ν/cm^{-1})	168 K (ν/cm^{-1})	150 K ν/cm^{-1}	100 K ν/cm^{-1}	Tentative assignments
3262 m sh	3264 ms	3273 ms	3275 ms	3280 mw	ν_{NH} (in weak hydrogen bonds 2.99–3.14 Å)
3208 sh	3214 bd	3210 s bd	3210 s bd	3197 mw	
3133 vs	3117 vs	3118 vs	3120 vs	3119 sh	ν_{NH} (in medium hydrogen bonds 2.88–2.09 Å)
				3095 vs	ν_{NH} (in strong hydrogen bonds N–H $\cdots$ F $\leq$ ~ 2.82 Å)
—	3083 sh	3082 sh	3082 s	3084 vs	
				3066 vs	
—	—	—	—	3026 W	

Note. m: medium; ms: medium sharp; mw: medium weak; bd: broad; s: sharp, vs: very sharp; sh: shoulder; w: weak; vw: very weak. The modes observed below 3000 cm^{-1} are due to overtones and combination tones.

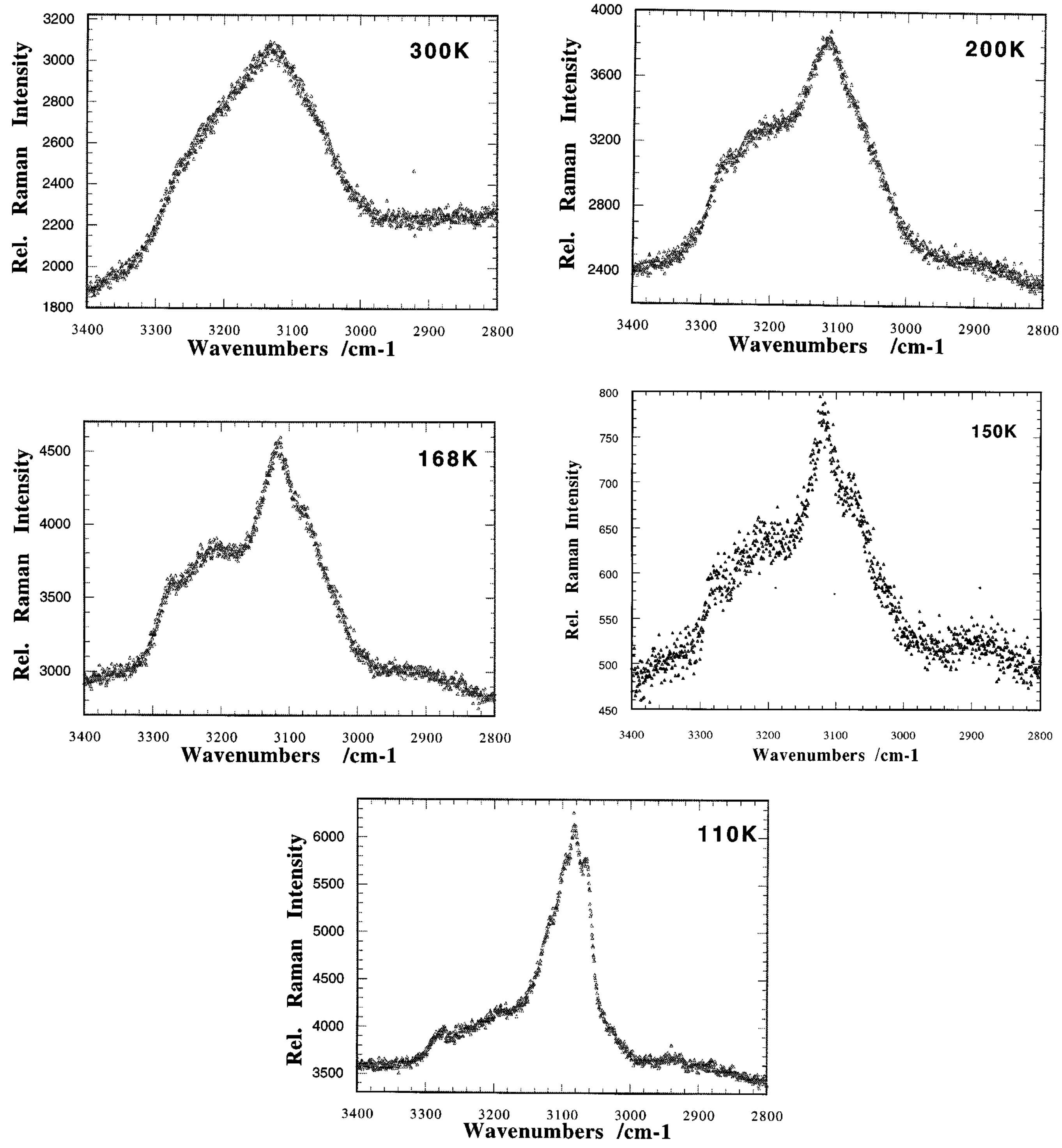

FIG. 6. High frequency domains of the Raman spectra of β-$(NH_4)_2FeF_5$ recorded between 300 and 100 K.

change in the octahedron bridging angle. This results in a sudden change in the chain length versus temperature curve and explains the break in the cell parameters versus temperature curves. From the powder study, it is not possible to determine whether a different cell and/or space group is to be considered for low temperature β-$(NH_4)_2FeF_5$. A previous Mössbauer study (7) has shown that the local environment of the iron atoms changes at low temperature: in the temperature range 200–150 K, the iron sites are not structurally equivalent as it is the case at room temperature. This change was attributed to a structural transition. In fact, two well distinct iron sites had to be taken into account at very low temperature to refine the magnetic data (site 1 at 20% and site 2 at 80%). The presence of two nonequivalent magnetic iron sites is related to a nonequivalence of the interchain pathways which allows the cooperative 3D magnetic ordering. The freezing out of an ammonium group, evidenced in this work, confirms this hypothesis by allowing stronger magnetic interaction pathways. Also, the question arises of why the second NH_4^+ group does not order at low temperature whereas the first group does so at about 193 K. Further ordering could be found at lower temperature but it may also be that the second ammonium group presents a static disorder that is not leading to a rearrangement at low temperature.

Additional spectroscopic work using isotopic H/D dilution should provide more detailed information about the ordering mechanism.

REFERENCES

1. V. Bentrup and L. Kolditz, *J. Therm. Anal.* **33,** 827 (1988).
2. J. L. Fourquet, A. LeBail, H. Duroy, and M. C. Moron, *Eur. J. Solid State Inorg. Chem.* **26,** 435 (1989).
3. P. Deniard, M. Evain, J. M. Barbet, and R. Brec, *in* "Materials Science Forum," p. 79. Trans Tech Publications, 1991.
4. J. Rodriguez-Carvajal, *Physica B* **192,** 55 (1993).
5. GSAS, A. L. Larson, and R. B. von Dreele, "LANSCE MS-H805." LANL, 1985–1994.
6. K. Nakamoto, "Infrared and Raman Spectra of Inorganic and Coordination Compounds," 3rd ed. Wiley, New York (1978).
7. Y. Calage, M. C. Moron, J. L. Fourquet, and F. Palacio, *J. Magn. Magn. Mater.* **98,** 79 (1991).